Published in final edited form as:
Neurol Sci. 2009 December ; 30(6): 471–477. doi:10.1007/s10072-009-0135-6.

Size frequency distribution of the *β*-amyloid (a*β*) deposits in dementia with Lewy bodies with associated Alzheimer's disease pathology

Richard A. Armstrong and
Vision Sciences, Aston University, Birmingham B4 7ET, UK

Nigel J. Cairns
Department of Neurology, Washington University School of Medicine, St Louis, MO 63110, USA; Department of Pathology and Immunology, Washington University School of Medicine, St Louis, MO 63110, USA

Abstract

The objective is to study *β*-amyloid (A*β*) deposition in dementia with Lewy bodies (DLB) with Alzheimer's disease (AD) pathology (DLB/AD). The size frequency distributions of the A*β* deposits were studied and fitted by log-normal and power-law models. Patients were ten clinically and pathologically diagnosed DLB/AD cases. Size distributions had a single peak and were positively skewed and similar to those described in AD and Down's syndrome. Size distributions had smaller means in DLB/AD than in AD. Log-normal and power-law models were fitted to the size distributions of the classic and diffuse deposits, respectively. Size distributions of A*β* deposits were similar in DLB/AD and AD. Size distributions of the diffuse deposits were fitted by a power-law model suggesting that aggregation/disaggregation of A*β* was the predominant factor, whereas the classic deposits were fitted by a log-normal distribution suggesting that surface diffusion was important in the pathogenesis of the classic deposits.

Keywords

Dementia with Lewy bodies (DLB); Alzheimer's disease (AD); *β*-Amyloid (A*β*) deposits; Size frequency distributions; Log-normal model; Power-law model

Introduction

The deposition of *β*-amyloid (A*β*) in the form of diffuse ('pre-amyloid'), primitive ('neuritic'), and classic ('densecored') deposits is one of the pathological hallmarks of Alzheimer's disease (AD) and Down's syndrome (DS) [1]. In AD and DS, A*β* deposits up to 150 μm in diameter can be observed in single sections of the cerebral cortex [2-4]. The frequency distributions of A*β* deposit size in AD and DS have a single peak (unimodal) and are positively skewed, i.e. there are few deposits in the smallest size classes (<10 μm), maximum frequency occurs between deposit diameters of 20 and 40 μm (the modal class), and the frequency of the larger deposits declines exponentially with increasing size [2-4]. The size frequency distributions of the A*β* deposits provide information on two aspects of AD pathology: (1) a more accurate

R.A.Armstrong@aston.ac.uk.

measure of neuronal damage than density measurements [5,6], and (2) the pathogenesis of the deposits [2,3].

A statistical mechanics approach has been adopted to model the growth of Aβ deposits in AD [7,8]. Two major processes have been identified: (1) addition and removal of protein molecules ('aggregation/disaggregation') and (2) diffusion of substances into a deposit ('surface diffusion') [7]. During aggregation, monomers of Aβ interact with each other to form more complex oligomers resulting in growth of the deposit. By contrast, during disaggregation, Aβ molecules are removed from a deposit by glial cells resulting in the shrinkage and ultimately the clearance of a deposit. Hence, positive growth of an Aβ deposit occurs when there is an imbalance between the processes of aggregation and disaggregation. By contrast, 'surface diffusion' is a process by which additional molecular constituents are acquired by a protein deposit by diffusion from the brain parenchyma [8,9]. Several proteins are known to be incorporated into Aβ deposits in AD including amyloid-P, α-antichymotrypsin, complement factors [10], and apolipoprotein E (Apo E) [11], and these additional constituents may influence deposit growth and morphology. The processes of aggregation/disaggregation and surface diffusion have a predictable effect on the size frequency distributions of the resulting Aβ deposits [2,8]. Hence, the frequency distribution of the Aβ deposits can be described by a 'power-law' function if the processes of aggregation/disaggregation predominate over those of surface diffusion and a 'log-normal' model if surface diffusion is the predominant factor [8].

Aβ deposits also occur in a significant number of cases of dementia with Lewy bodies (DLB) [12-14]. DLB is characterised pathologically by the presence of α-synuclein positive Lewy bodies (LB) in the brain stem and/or cortical and limbic regions [15]. In some cases, the density of cortical Aβ deposits may be similar to that of AD [12-14]. These cases are often described as 'mixed' cases of DLB (DLB/AD) or the Lewy body variant (LBV) of AD and combine many of the features of DLB and AD [16]. Hence, the objectives of the present study were to determine in DLB/AD: (1) whether the size distributions of the diffuse, primitive, and classic Aβ deposits in the temporal lobe were similar to those described previously in 'pure' AD [2, 3,17] and (2) whether a log-normal distribution or a power-law model could account for the size distributions.

Materials and methods

Cases

Brain tissue from ten male cases of DLB/AD was obtained from the Brain Bank, Department of Neuropathology, Institute of Psychiatry, King's College London, UK (Table 1). Cases were not a random selection of the DLB cases available but were chosen for their high densities of Aβ deposits. There is a gender imbalance in DLB towards males [15] but the all male sample is a reflection of the small number of cases employed in the study. A summary of the clinical features at presentation and occurring during the course of the disease together with the mini-mental status exam (MMSE) score at death are given in Table 2. Memory impairments were observed at presentation in 7/10 patients and significant Parkinson's disease (PD) symptoms were present at some stage of the disease in 5/10 patients. Disease onset was identified as the time the first symptoms of the disease appeared and not the appearance of dementia. After death, the consent of the next of kin was obtained for brain removal, following local Ethical Committee procedure and the 1995 Declaration of Helsinki (as modified Edinburgh, 2000). DLB cases were diagnosed according to the 'Consortium on Dementia with Lewy bodies' (CDLB) guidelines [15]. In addition, all cases had sufficient densities of Aβ deposits (Table 1) for a diagnosis of DLB/AD according to the 'Consortium to Establish a Registry of Alzheimer's disease' (CERAD) criteria [18]. These cases also had significant numbers of cortical neurofibrillary tangles (NFT) (Table 1). Size frequency distributions of Aβ deposits

in DLB/AD were compared with previously published data for ten cases of sporadic AD [3, 4,17]. The mean age at death of AD cases (3 male:7 female) was 81.8 years (SD = 8.51), mean duration of disease was 7.0 years (SD = 3.31), and the MMSE at death was in the range 0–5).

Tissue preparation

A block of the temporal lobe, at the level of the lateral geniculate body, was taken from each case and included the inferior temporal gyrus (ITG), lateral occipitotemporal gyrus (LOT), the parahippocampal gyrus (PHG), hippocampus (HC), and dentate gyrus (DG). Tissue was fixed in 10% phosphate buffered formal-saline and embedded in paraffin wax; 7 μm coronal sections were stained with a rabbit polyclonal antibody (Gift of Prof. B.H. Anderton, Institute of Psychiatry, King's College London) raised to the 12–28 amino acid sequence of the Aβ protein [19]. The antibody was used at a dilution of 1 in 1,200 and the sections incubated at 4°C overnight. Sections were pretreated with 98% formic acid for 6 min which enhances Aβ immunoreactivity. Aβ was visualised using the streptavidin–biotin horseradish peroxidase procedure with diaminobenzidine as the chromogen. Sections were also stained with haematoxylin. Aβ deposits are usually divided into three subtypes [20,21]: (1) diffuse deposits are 10–200 μm in diameter, lightly stained, irregular in shape, and with diffuse boundaries, (2) primitive deposits are 20–60 μm, well demarcated, symmetrical in shape, and strongly stained, and (3) classic deposits are 20–100 μm had a distinct amyloid core surrounded by a 'corona' in which Aβ is located adjacent to dystrophic neurites.

Morphometric methods

In the ITG, LOT, and PHG, randomly located guidelines were marked on the slide extending from the pia mater to the white matter. The greatest diameter of all Aβ deposits, greater than 5 μm in diameter, and which touched a guideline, were measured at ×400 using an eyepiece micrometer. In the HC, all deposits from sectors CA1 to CA4 inclusive were measured and in the DG, all deposits within the molecular layer. Data from the ten cases were combined to construct a size frequency distribution of the diffuse, primitive, and classic Aβ deposits for each brain region.

Data analysis

A log-normal distribution and a power-law function were fitted to the size distributions using STATISTICA software (Statsoft Inc., 2300 East 14th St, Tulsa, OK 74104, USA). First, the log-normal distribution was fitted to each size distribution and is defined as that of a variable X such that $\ln(X - Ø)$ is normally distributed. This distribution has three parameters: a constant Ø (where $X > Ø$), the mean μ, and the variance r^2. In many applications, the value of Ø can be assumed to be zero and a two-parameter model fitted to the data. Deviations from a log-normal model were tested using the Kolmogorov–Smirnov (KS) goodness of fit test. Second, a variable (Y) is distributed as a power-law function of X if the dependent variable has an exponent a, i.e. a function of the form $Y = CX^{-a}$. If a function of this type fits the data, a plot of log Y against log X should yield a linear relationship. Hence, Aβ deposit sizes were grouped into size classes and the log of the frequency of the Aβ deposits in each class plotted against the log of the upper size limit of the size class. A linear regression was fitted to the data and the goodness of fit to a linear model tested using Pearson's correlation coefficient (r). In addition, χ^2 contingency table tests were used to compare the size frequency distributions of Aβ deposits between different regions of the temporal lobe [6]. The degree of correlation (Pearson's r) was also calculated between the modal size class of the Aβ deposits in cortical, hippocampal, and dentate gyrus regions of the individual patients and disease duration.

Results

The size frequency distributions of the diffuse and classic Aβ deposits in the LOT in DLB/AD are shown in Figs. 1 and 2. Both distributions had a single peak and exhibited a significant degree of positive skew, i.e. with the mode to the left ($P < 0.01$). There were few deposits in the smallest size class, the mode occurred at an upper size class limit of approximately 40 μm for the diffuse deposits (Fig. 1) and 30 μm for the classic deposits (Fig. 2), and the frequency of the larger deposits declined with increasing size.

The distribution statistics for all the Aβ populations studied is shown in Table 3. All size distributions were unimodal and, with the exception of the classic Aβ deposits in the ITG, exhibited a significant degree of positive skew. Differences in size distributions were apparent both between deposit subtypes and brain region. First, in the ITG, LOT, and PHG, and CA sectors of the HC, the primitive deposits had smaller means and were less skewed than the diffuse and classic deposits. Second, the distribution of the diffuse deposits in the CA sectors of the HC had a larger mean and was more significantly skewed than in the ITG and LOT. Third, the size distributions of the primitive deposits in the CA sectors and DG molecular layer had larger means and were more skewed than in the ITG, LOT, and PHG.

Figures 1 and 2 also show the fitted log-normal distributions. The observed size distribution of the diffuse deposits (Fig. 1) deviated significantly from a log-normal model (KS = 0.10, $P < 0.01$). There were fewer diffuse deposits in size classes smaller than the mode, more in the modal class, and fewer larger than the mode than expected from the model. The distribution of the classic deposits (Fig. 2) did not deviate significantly from a log-normal model (KS = 0.09, $P > 0.05$). An example of fitting the power-law model to the size distribution of the diffuse deposits in the LOT is shown in Fig. 3. There was a significant linear decline in log frequency with log size class ($r = -0.75$, $P < 0.01$) suggesting the size distribution did not deviate significantly from a power-law model.

The results of fitting the log-normal distribution and power-law function to data from all brain regions is shown in Table 4. The frequency distributions of the diffuse and primitive deposits in the ITG, LOT, and PHG deviated significantly from a log-normal model, whereas the frequency distribution of the classic deposits was consistent with a log-normal model. In addition, the diffuse deposits in the ITG, LOT and PHG and the primitive deposits in the CA sectors of the hippocampus were fitted successfully by a power-law function.

The degree of correlation (Pearson's r) between the modal size class of the Aβ deposits in cortical, hippocampal, and dentate gyrus regions of individual patients, and disease duration is shown in Table 5. Modal size class of the diffuse and classic deposits was positively correlated with duration of disease in cortical regions and the hippocampus, respectively. By contrast, the primitive and classic deposits were not significantly correlated with disease duration in the cortex and the diffuse and primitive deposits were either not significantly correlated or possibly even negatively correlated with disease duration in the CA sectors of the hippocampus.

Discussion

The first objective was to determine whether the size distributions of Aβ deposits in DLB/AD were similar to those in AD. A summary of the size frequency distributions of Aβ deposits for the previously published AD group [3,4,17] is given in Table 6. Comparison between groups is complicated by the differences in mean age and especially gender distribution in the AD and DLB/AD groups and because the DLB cases were not a random sample of those available. In particular, the DLB group comprises all males while the AD group has a mixture of males and females. Furthermore, the all male DLB sample reflects the lack of representativeness of the

sample and not the fact that females with DLB have less Aβ deposition. In addition, although the two groups have similar duration of disease (mean duration 8 years, SD = 6.0) compared with AD (mean duration 7 years, SD = 3.3), disease onset in the DLB/AD group represents the appearance of any of the symptoms characteristic of DLB and not the onset of dementia as in AD.

Nevertheless, the size distributions of the Aβ deposits in DLB/AD had similarities with those in AD. First, the size frequency distributions in DLB/AD were unimodal and positively skewed and similar in shape to those in AD [2,3,17]. Second, as in AD, the size distributions of the classic and diffuse deposits had larger means and exhibited a greater degree of skew than the primitive deposits. With the exception of the CA sectors of the HC, however, the size distributions in DLB/AD had smaller means than in AD. Although there is evidence that the rate of progression of disease may be faster in DLB than in AD [22], Aβ deposition might be associated with the onset of dementia and this may occur later in the course of the disease in DLB/AD.

The second objective was to determine whether a lognormal or a power-law model fitted the size distributions. In the ITG, LOT, and PHG a power-law model successfully fitted the size distributions of the diffuse deposits. In AD and DS, diffuse deposits aggregate around clusters of neuronal cell bodies [23-25]. Development of diffuse deposits may therefore involve first, secretion of Aβ monomers from clusters of adjacent neuronal perikarya; second, the association of Aβ monomers to form more complex oligomers, and third, the formation of an aggregated deposit [25,26]. Disaggregation within a developing deposit may also occur as a result of the removal of Aβ monomers by glial cells embedded within and present at the periphery of many diffuse deposits [27]. Hence, an imbalance between aggregation and disaggregation is likely to be the predominant factor in the formation of the diffuse deposits. The positive correlation between the size of the modal class of Aβ deposits in cortical areas and disease duration is consistent with growth of diffuse deposits over time. A successful fit to a power-law model also implies that surface diffusion was less important in diffuse deposits. Fewer additional molecular constituents have been recorded in diffuse compared with classic Aβ deposits in AD consistent with this suggestion [21].

In the ITG, LOT, and PHG, a log-normal model provided a more successful fit to the size distributions of the classic deposits as previously reported in AD and in DS [2]. In AD, the classic deposits often aggregate around the larger diameter arterioles and substances leaking from damaged blood vessels, may be incorporated into the deposits by surface diffusion [28]. A number of additional substances have been found within classic deposits including immunoglobulins, amyloid-P, α1-antichymotrypsin, antitrypsin, antithrombin III, complement factors and apo E consistent with diffusion [21]. Some of these substances may have ‘chaperone-like’ activity and influence the development of the deposit by enhancing the aggregation of Aβ monomers [29,30] or encouraging the condensation of the amyloid to form a dense core [21].

In the ITG, LOT, and PHG neither the log-normal nor power-law models fitted the size distributions of the primitive deposits. By contrast, in the CA sectors of the hippocampus, the size distribution of the primitive deposits was fitted by a power-law model while in the molecular layer of the dentate gyrus, both models provided a fit to the data. Hence, the pathogenesis of the primitive deposits appears to be complex and both aggregation/disaggregation and surface diffusion, together with currently unidentified factors involved in pathogenesis.

Modal size class of the diffuse and classic deposits was positively correlated with duration of disease in cortical regions and the hippocampus, respectively. By contrast, the primitive and

classic deposits were not significantly correlated with disease duration in the cortex and the diffuse and primitive deposits were either not significantly correlated or possibly even negatively correlated with disease duration in the CA sectors of the hippocampus. These results suggest that the pattern of growth and development of the Aβ deposits depends both on deposit type and brain region. Hence, the best evidence for growth of deposits over time is shown by the diffuse deposits in the cortex and classic deposits in the hippocampus. By contrast, the size of the primitive deposits was not significantly correlated with duration in any of the brain regions studied and may even be negatively correlated. It is possible that the primitive deposits are formed much more rapidly than the diffuse and classic types and once formed change little or even shrink in size with time.

In conclusion, the size distributions of Aβ deposits in cases of DLB/AD were unimodal and positively skewed and similar, apart from a smaller mean size, to those of AD. Size distributions of the diffuse deposits were fitted by a power-law model suggesting that aggregation/disaggregation of Aβ was the predominant factor, whereas the classic deposits were fitted by a log-normal distribution suggesting that surface diffusion was important.

Acknowledgments

The assistance of the Brain Bank, Institute of Psychiatry, King's College London, UK, in providing tissue sections for this study is gratefully acknowledged. We would like to thank Mr Andrew Chadwick and Mrs Mavis Kibble for their excellent technical assistance.

References

1. Glenner GG, Wong CW. Alzheimer's disease and Down's syndrome: sharing of a unique cerebrovascular amyloid fibril protein. Biochem Biophys Res Commun 1984;122:1131–1135. [PubMed: 6236805]
2. Hyman BT, West HL, Rebeck GW, et al. Quantitative analysis of senile plaques in Alzheimer's disease: observation of log-normal size distributions associated with apolipoprotein E genotype and trisomy 21 (Down's syndrome). Proc Natl Acad Sci USA 1995;92:3586–3590. [PubMed: 7724603]
3. Armstrong RA. Do β-amyloid (Aβ) deposits in patients with Alzheimer's disease and Down's syndrome grow according to the log-normal model? Neurosci Lett 1999;261:97–100. [PubMed: 10081936]
4. Armstrong RA, Myers D, Smith CUM. Factors determinng the size frequency distribution of β-amyloid (Aβ) deposits in Alzheimer's disease. Exp Neurol 1997;145:574–579. [PubMed: 9217093]
5. Armstrong RA. Quantifying the pathology of neurodegenerative disorders: quantitative measurements, sampling strategies, and data analysis. Histopathology 2003;42:521–529. [PubMed: 12786887]
6. Armstrong RA, Myers D, Smith CUM. Alzheimer's disase: size class frequency distributions of senile plaques: do they indicate when a brain region was affected? Neurosci Lett 1991;127:223–226. [PubMed: 1881634]
7. Stanley HE, Buldyrev SV, Cruz L, et al. Statistical physics and Alzheimer's disease. Physica A 1998;249:460–471.
8. Urbanc B, Cruz L, Buldyrev SV, et al. Dynamics of plaque formation in Alzheimer's disease. Biophys J 1999;76:1330–1334. [PubMed: 10049316]
9. Armstrong RA, Lantos PL, Cairns NJ. What determines the molecular composition of abnormal protein aggregates in neurodegenerative disease. Neuropathology 2008;28:351–365. [PubMed: 18433435]
10. Kalaria, RN.; Kroon, SN.; Perry, G. Adv Biosc. Vol. 87. 1993. Serum proteins and the blood-brain barrier in the pathogenesis of Alzheimer's disease; p. 282In: Nicolini M, Zarta PF, Corain B (eds) Alzheimer's disease and related disorders
11. Saunders AM, Strittmatter WJ, Schmechel D, et al. Association of apolipoprotein E allele e4 with late-onset familial and sporadic Alzheimer's disease. Neurology 1993;43:1467–1472. [PubMed: 8350998]

12. Gibb WRG, Luthert PJ, Janota I, et al. Cortical Lewy body dementia: clinical features and classification. J Neurol Neurosurg Psychiatr 1989;52:185–192. [PubMed: 2467966]
13. Dickson DW, Ruan D, Crystal H, et al. Hippocampal degeneration differentiates diffuse Lewy body disease (DLBD) from Alzheimer's disease: light and electron microscope immunocytochemistry of CA2–3 neurites specific to DLBD. Neurology 1991;41:1402–1409. [PubMed: 1653914]
14. Armstrong RA, Cairns NJ, Lantos PL. The spatial patterns of Lewy bodies, senile plaques and neurofibrillary tangles in dementia with Lewy bodies. Exp Neurol 1998;150:122–127. [PubMed: 9514834]
15. McKeith IG, Galasko D, Kosaka K, et al. Consensus guidelines for the clinical and pathological diagnosis of dementia with Lewy bodies (DLB): report of the consortium on DLB international workshop. Neurology 1996;47:1113–1124. [PubMed: 8909416]
16. Armstrong RA. The interface between Alzheimer's disease, normal aging and related disorders. Curr Aging Sci 2008;1:122–132. [PubMed: 20021381]
17. Armstrong RA. Size distribution curves of senile plaques in patients with Alzheimer's disease: do plaques grow according to the log-normal model? Alzheimer Res 1997;3:63–67.
18. Mirra SS, Heyman A, McKeel D, et al. The consortium to establish a registry for Alzheimer's disease (CERAD). II Standardization of the neuropathological assessment of Alzheimer's disease. Neurology 1991;41:479–486. [PubMed: 2011243]
19. Spargo E, Luthert PJ, Janota I, et al. β/A4 deposition in the temporal cortex of adults with Down's syndrome. J Neurol Sci 1992;111:26–32. [PubMed: 1402995]
20. Delaere P, Duyckaerts C, He Y, et al. Subtypes and differential laminar distribution of β/A4 deposits in Alzheimer's disease: relationship with the intellectual status of 26 cases. Acta Neuropathol 1991;81:328–335. [PubMed: 1711758]
21. Armstrong RA. β-amyloid plaques: stages in life history or independent origin? Dement Geriatr Disord 1998;9:227–238.
22. Olichney JM, Hansen LA, Galasko D, et al. The apolipoprotein E epsilon 4 allele is associated with neuritic plaques and cerebral amyloid angiopathy in Alzheimer's disease and Lewy body variant. Neurology 1996;47:190–196. [PubMed: 8710076]
23. Allsop D, Haga S, Ikeda SI, et al. Early senile plaques in Down's syndrome brains show a close relationship with cell bodies of neurons. Neuropathol Appl Neurobiol 1989;15:531–542. [PubMed: 2559339]
24. Miyakawa T, Katsuragi S, Yamashiba K, et al. Morphological study of amyloid fibrils and preamyloid deposits in the brain with Alzheimer's disease. Acta Neuropathol 1992;83:340–346. [PubMed: 1575011]
25. Armstrong RA. Diffuse β-amyloid (Aβ) deposits and neurons: in situ secretion or diffusion of Aβ. Alzheimer Rep 2001;3:289–294.
26. Benes FM, Reifel JL, Majocha RE, et al. Evidence for a diffusional model of Alzheimer amyloid A4 (β-amyloid) deposition during neuritic plaque formation. Neuroscience 1989;33:483–488. [PubMed: 2700016]
27. Armstrong RA, Cairns NJ, Lantos PL. Degeneration of cortical neurons associated with diffuse β-amyloid (Aβ) deposits in Alzheimer's disease. Neurosci Res Communs 1999;24:89–97.
28. Armstrong RA. Classic β-amyloid deposits cluster around large diameter blood vessels rather than capillaries in sporadic Alzheimer's disease. Curr Neurovasc Res 2006;3:289–294. [PubMed: 17109624]
29. Ma J, Yee A, Brewer B, et al. Amyloid-associated proteins β1-antichymotrypsin and apolipoprotein e promote assembly of Alzheimer β-protein into filaments. Nature 1994;372:92–94. [PubMed: 7969426]
30. Kuner P, Bohrmann B, Tjernberg LO, et al. Controlling polymerization of beta-amyloid and prion-derived protein with synthetic small molecular ligands. J Biol Chem 2000;275:1673–1678. [PubMed: 10636861]

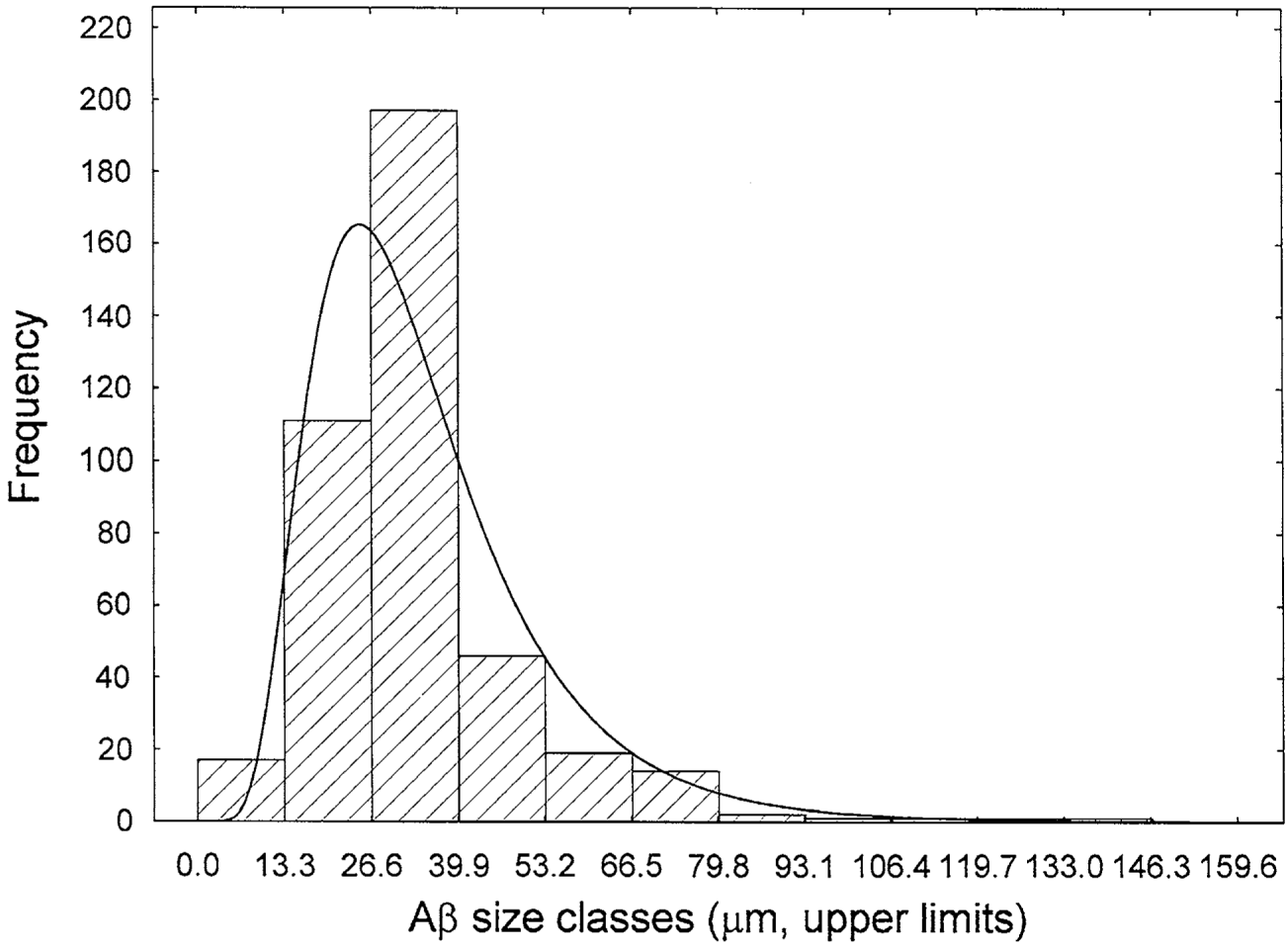

Fig. 1.

The size frequency distributions of the diffuse *β*-amyloid (A*β*) deposits in the lateral occipitotemporal gyrus (LOT) in a case of dementia with Lewy bodies with associated Alzheimer's disease pathology. The fitted curve represents the log-normal distribution (KS = 0.10, $P < 0.05$)

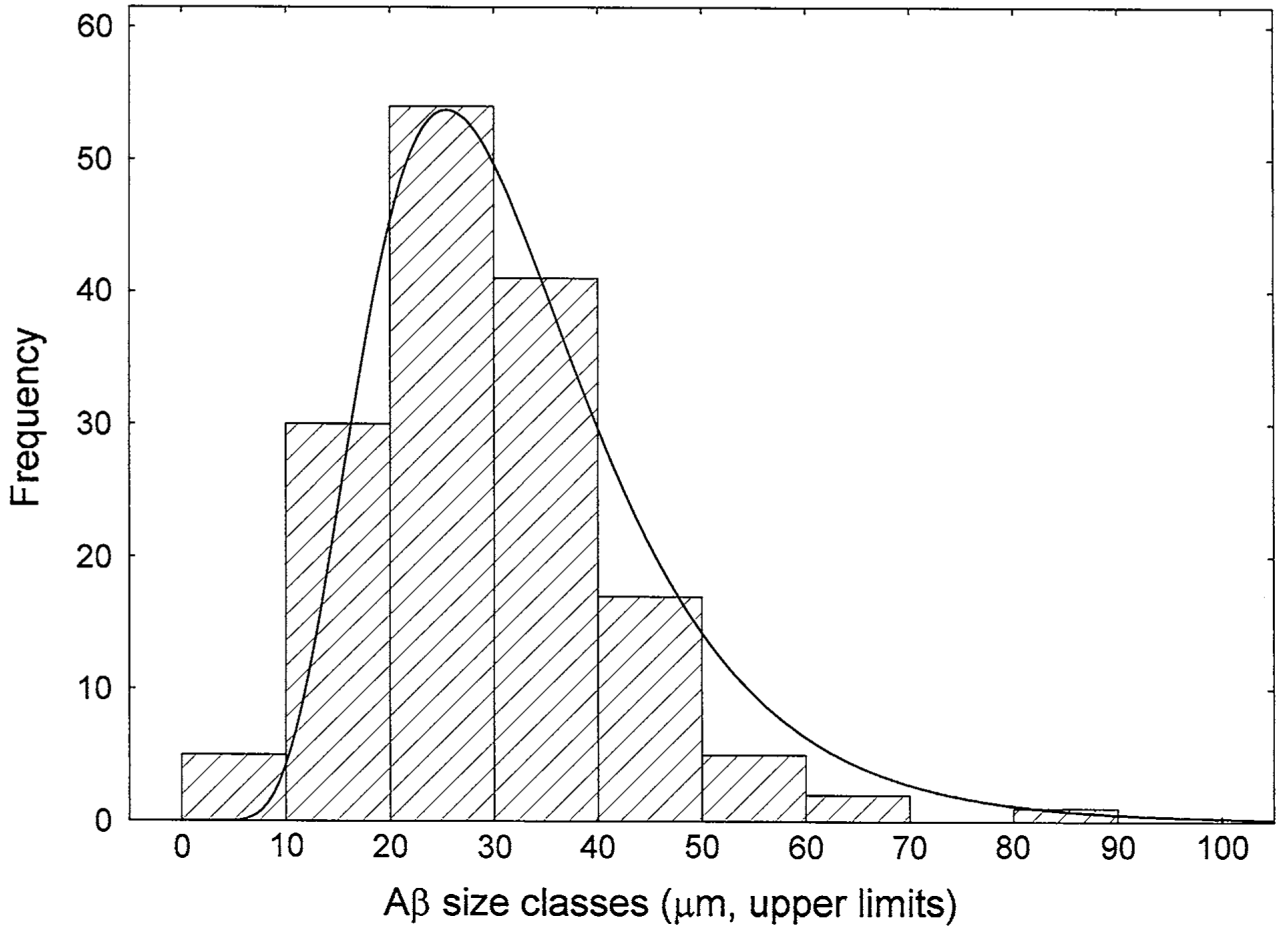

Fig. 2.

The size frequency distributions of the classic *β*-amyloid (A*β*) deposits in the lateral occipitotemporal gyrus (LOT) in a case of dementia with Lewy bodies with associated Alzheimer's disease pathology. The fitted curve represents the log-normal distribution (KS = 0.09, $P > 0.05$)

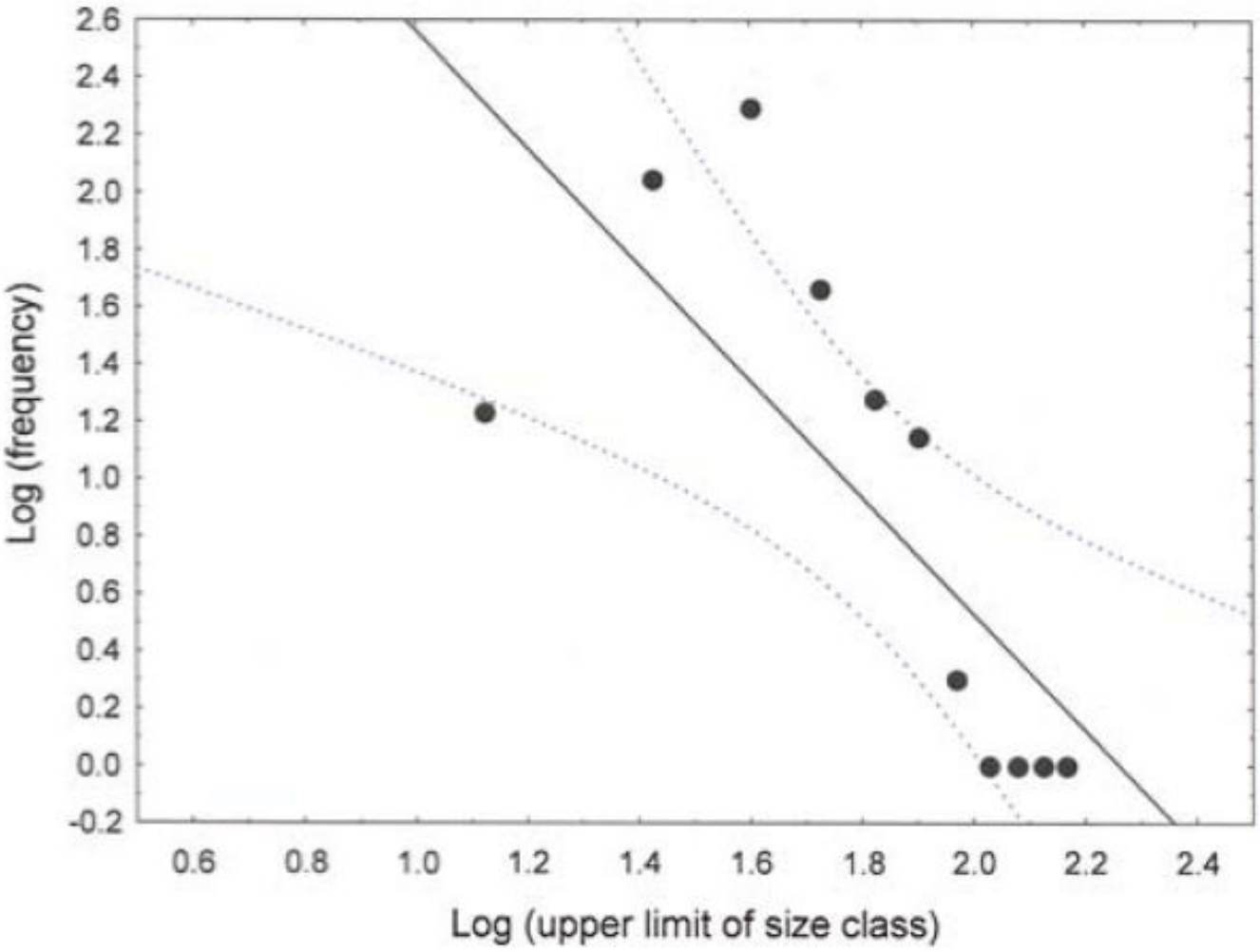

Fig. 3.
Goodness of fit of the diffuse β-amyloid (Aβ) deposits in the lateral occipitotemporal gyrus (LOT) to a power-law model ($r = -0.75$, $P < 0.01$)

Table 1

Demographic data, cause of death, and overall lesion densities in the dementia with Lewy body (DLB) cases studied

Case	Gender	Onset	Age	Cause of death	LB	SP	NFT
E	M	73	77	Empyema	9.6	7.2	1.9
F	M	NA	72	Shock/hypothermia	2.6	19.2	1.2
G	M	NA	76	Acute renal failure	8.3	10.3	3.8
H	M	NA	69	Bronchopneumonia	7.0	13.1	1.7
I	M	67	82	Bronchopneumonia	1.1	13.1	2.1
J	M	51	58	Bronchopneumonia	3.7	23.7	1.2
K	M	79	83	Myocardial infarction	7.8	10.2	4.5
L	M	68	71	Bronchopneumonia	8.0	6.8	0.5
M	M	64	82	NA	5.4	9.8	3.1
N	M	65	70	Bronchopneumonia	3.8	10.1	2.7

Column 6 shows mean cortical densities per mm^2 of α-synuclein positive Lewy bodies (LB) and columns 7 and 8, densities of senile plaques (SP) and neurofibrillary tangles (NFT) revealed by the Bielschowsky silver impregnation method

M Male, *NA* data not available

Table 2

Summary of the clinical features in the dementia with Lewy bodies (DLB) cases with associated Alzheimer's disease (AD) pathology (DLB/AD) at presentation and during the course of the disease

Case	At presentation	During disease	MMSE
A	Memory impairment	Apathy, PD symptoms	1
B	Memory impairment	Visuo-spatial problems dementia	3
C	Visual hallucinations	Disorientation, paranoia, dementia	1
D	Memory impairment	Dementia	2
E	PD symptoms	Memory impairment, dementia	1
F	Memory impairment	Visuo-spatial problems, confusion, dementia	0
G	Personality change, memory impairment	Paranoid delusions, dementia, PD symptoms	2
H	Memory impairment, confusion	Typical AD dementia PD symptoms	0
I	PD symptoms	Memory impairment, visual hallucinations	0
J	Language difficulties	Visuo-spatial problems, confusion, dementia	0

MMSE Mini-mental status exam prior to death, *PD* Parkinson's disease

Table 3

Size frequency distribution statistics of the diffuse (D), primitive (P) and classic (CL) β-amyloid (Aβ) deposits in the temporal lobe of patients with dementia with Lewy bodies (DLB) with associated Alzheimer's disease (AD) pathology (DLB/AD)

Region	Aβ	N	Median	Mode	Mean	SD	Skew
ITG	D	339	30	30	32.14	14.5	0.84**
	P	130	20	20	21.50	10.32	0.87**
	CL	81	30	30	30.24	13.92	0.41 (NS)
LOT	D	410	30	30	34.72	17.74	1.79**
	P	255	20	20	24.35	10.28	0.71**
	CL	155	30	30	32.74	12.90	0.88**
PHG	D	369	40	30	39.50	19.64	1.72**
	P	215	20	10	23.70	12.25	0.88**
	CL	117	40	40	40.64	16.81	0.83**
HC	D	217	40	40	42.07	21.31	1.35**
	P	202	30	M	30.59	17.22	1.48**
	C	25	40	40	39.20	22.89	0.93**
DG	P	119	30	30	28.82	12.31	0.79**

ITG Inferior temporal gyrus, *LOT* lateral occipitotemporal gyrus, *PHG* parahippocampal gyrus, *HC* hippocampus (CA1–CA4), *DG* Dentate gyrus, *N* number of deposits sampled, *DF* degrees of freedom, *NS* not significant

Chi-square (χ^2) contingency table tests comparing size frequency distributions: (A) within each brain region, *D* versus *P* χ^2 = 62.99 (8 *DF*, *P* < 0.001), *D* versus *CL* χ^2 = 6.85 (8 *DF*, *P* > 0.05), *P* versus *CL* χ^2 = 42.04 (5 *DF*, *P* < 0.001); *LOT D* versus *P* χ^2 = 85.45 (8 *DF*, *P* < 0.001), *D* versus *CL* χ^2 = 8.97 (8 *DF*, *P* > 0.05), *P* versus *CL* χ^2 = 43.99 (*P* < 0.001); *PHG D* versus *P* χ^2 = 126.83 (8 *DF*, *P* < 0.001), *D* versus *CL* χ^2 = 3.23 (8 *DF*, *P* > 0.05), *P* versus *CL* χ^2 = 85.28 (8 *DF*, *P* < 0.001); *HC D* versus *P* χ^2 = 45.23 (8 *DF P* < 0.001). (B) between different brain regions, diffuse deposits *LOT* versus *PHG* χ^2 = 8.89 (8 *DF*, *P* > 0.05), *ITG* versus *HC* χ^2 = 48.49 (8 *DF*, *P* < 0.001), *LOT* versus *HC* = 20.48 (8 *DF*, *P* < 0.01), *PHG* versus *HC* χ^2 = 6.71 (8 *DF*, *P* > 0.05); primitive deposits, between cortical regions χ^2 = 22.18 (12 *DF*, *P* > 0.05), *HC* versus *DG* χ^2 = 7.99 (8 *DF*, *P* > 0.05) total for cortical gyri versus *HC* + *DG* χ^2 = 62.56 (*DF*, *P* < 0.001), classic deposits, *ITG* versus *PHG* χ^2 = 14.38 (8 *DF*, *P* > 0.05), *ITG* versus *LOT* χ^2 = 4.18 (7 *DF*, *P* > 0.05), *PHG* versus *LOT* χ^2 = 22.56 (8 *DF*, *P* < 0.01)

** *P* < 0.01

Table 4

Size class frequency distributions of *β*-amyloid (A*β*) deposits in dementia with Lewy bodies with associated Alzheimer's disease (AD) pathology (DLB/AD)

Brain region	A*β* subtype	Dev. from log-normal model (KS)	Fit to power-law model ('r')
ITG	Diffuse	0.11**	−0.80*
	Primitive	0.17**	−0.69 (NS)
	Classic	0.12 (NS)	−0.68 (NS)
LOT	Diffuse	0.10**	−0.75**
	Primitive	0.13**	−0.66 (NS)
	Classic	0.09 (NS)	−0.57 (NS)
PHG	Diffuse	0.11**	−0.67*
	Primitive	0.18**	−0.56 (NS)
	Classic	0.09 (NS)	−0.13 (NS)
HC	Diffuse	0.08 (NS)	−0.54 (NS)
	Primitive	0.11**	−0.78**
DG	Primitive	0.10 (NS)	−0.78*

Fit to log-normal and power-law functions in each brain region

ITG Inferior temporal gyrus

LOT lateral occipitotemporal gyrus, *PHG* parahippocampal gyrus, *HC* hippocampus (CA1–CA4), *DG* dentate gyrus, *KS* Kolmorogorov–Smirnov statistic, *r* = Pearson's correlation coefficient, *NS* not significant

* $P < 0.05$;

** $P < 0.01$

Table 5

Correlations (Pearson's *r*) between the modal size class of the A*β* deposits in cortical, hippocampal, and dentate gyrus regions of individual patients and disease duration

***X* variable**	**A*β* deposit**	**Cortex**	**Hippocampus**	**Dentate gyrus**
Disease	Diffuse	0.49*	−0.53	-
Duration	Primitive	−0.21	−0.49	−0.40
	Classic	0.34	0.88**	-

*$P < 0.05$

**$P < 0.01$

Table 6

Summary of data of the size frequency distribution of β-amyloid (Aβ) deposits in various brain regions in 10 cases of sporadic Alzheimer's disease (AD)

Region	Aβ deposit	Mean size	Median	Mode	SD	Skew
ITG	Diffuse	50.80	50	50	20.88	1.17**
	Primitive	29.43	30	30	10.89	0.63**
	Classic	36.07	35	30	15.10	0.99**
LOT	Diffuse	45.96	40	50	19.71	1.04**
	Primitive	30.71	30	30	11.28	0.34**
	Classic	37.09	35	30	12.66	0.46**
PHG	Diffuse	46.06	40	40	19.44	1.49**
	Primitive	34.16	30	30	12.53	0.88**
	Classic	38.67	40	30	15.45	0.98**
HC	Diffuse	48.85	50	50	19.01	0.66**
	Primitive	31.81	30	30	11.24	0.51**
	Classic	42.20	40	30	20.05	1.04**
DG	Diffuse	36.67	30	30	18.11	1.04**

ITG Inferior temporal gyrus, *LOT* lateral occipitotemporal gyrus, *PHG* parahippocampal gyrus, *HC* hippocampus CA1-CA4, *DG* dentate gyrus, *SD* standard deviation

** $P < 0.01$